Bubbles for a Class of Delay Differential Equations
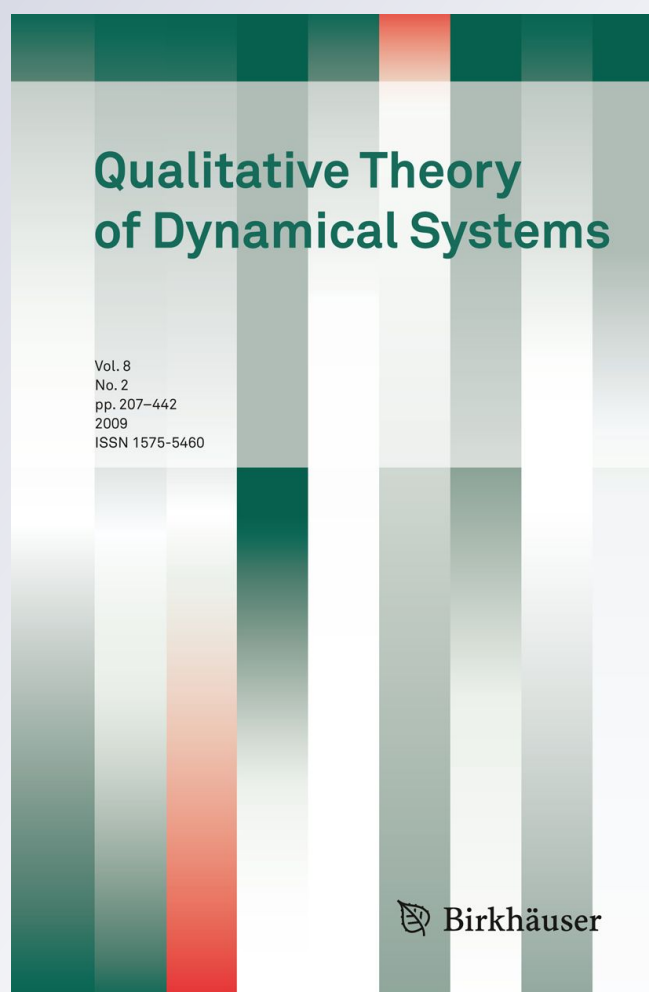
Tibor Krisztin & Eduardo Liz

Qualitative Theory
of Dynamical Systems

Vol. 8
No. 2
pp. 207–442
2009
ISSN 1575-5460

Birkhäuser

Springer

Springer

Bubbles for a Class of Delay Differential Equations

Tibor Krisztin · Eduardo Liz

Abstract　　We analyze the effect of increasing mortality in usual delayed recruitment models of the form $x'(t) = -\delta x(t) + f(x(t - \tau))$. We consider constant effort harvesting, and discuss the phenomenon of bubbling, which appears when for parameters δ in an interval I there exists a unique positive stationary point $K(\delta)$ in the phase space $C([-\tau, 0], \mathbb{R})$, and there exist $\delta_1 < \delta_2$ in I such that $K(\delta)$ is locally stable for $\delta \in I \backslash [\delta_1, \delta_2]$, and $K(\delta)$ is unstable for $\delta \in (\delta_1, \delta_2)$. We give a definition of bubbling in a more abstract setting, and show that it naturally appears in a variety of equations. For some nonlinearities rigorous proofs are available for the description of bubbles, for other nonlinearities we give numerical results to indicate the phenomenon of bubbling.

Keywords　　Delay differential equation · Periodic solutions · Nicholson's blowflies equation · Bubbling · Hopf bifurcation

Mathematics Subject Classification (2000)　　Primary 34K20; Secondary 34D45

1 Introduction

Many processes result from the interaction between production and destruction. Actually, there are a variety of biological systems (see, e.g., [16]) characterized by a time dependent quantity $x = x(t)$ in which the rate of change $x'(t)$ results from the balance

T. Krisztin
Bolyai Institute, University of Szeged, Aradi vértanúk tere 1, 6720 Szeged, Hungary
e-mail: krisztin@math.u-szeged.hu

E. Liz (✉)
Departamento de Matemática Aplicada II, E.T.S.I. Telecomunicación,
Universidad de Vigo, 36310 Vigo, Spain
e-mail: eliz@dma.uvigo.es

　　　　　　　　　　　　　　　　　　🕮 Birkhäuser

between the production rate and the destruction rate. In some cases, the production rate at a time t is a function of the quantity x at a previous time $t - \tau$, where τ is a maturation period. This leads to a simple delay-differential equation

$$x'(t) = -\delta x(t) + h(x(t - \tau)), \tag{1}$$

where δ is the destruction rate and h is the production function. Equation (1) has a long tradition, especially in population dynamics [4,6,12,19,30,31,34], and physiological processes [10,11,24–27].

In some situations, the destruction rate is a parameter that can be controlled, whereas the other parameters involved in the process are much more difficult to modify. A typical example is a model of population dynamics, where the destruction parameter δ means the mortality rate; thus, in a fishing or harvesting model, the mortality rate can be controlled by enhancing or reducing the harvesting effort [4,5,30,32].

One of the most famous examples of (1) in the framework of population dynamics is the *Nicholson's blowflies equation,* which has the form (1) with the recruitment function given by $h(x) = pxe^{-\gamma x}$, $p > 0$, $\gamma > 0$. This equation has been used by Gurney et al. [12] to explain the data obtained by Nicholson [33] in his famous experiments with Australian-sheep blowfly. If $x(t)$ represents the size of a population at time t, the delay parameter τ is a maturation time, and the positive coefficient δ stands for the mortality rate. In [34], a nice explanation is given for deriving Eq. (1) to model the growth of a structured population with two stages, juveniles and adults. In this case, δ stands for the adult per capita death rate.

Other well known example is the model of erythropoiesis introduced by Mackey [24] (see also [10]), who examined the role of peripheral red blood cells (RBC) destruction rate on the onset of auto-immune hemolytic anemia in rabbits. The delay differential equation (1) was used to model the rate of change of the circulating density of RBC. In this case, the parameter δ is the peripheral RBC destruction rate, and can be increased by administration of RBC antibodies. A monotone decreasing Hill function is used for the production rate.

These examples show that it is natural to use δ as a bifurcation parameter in (1) in order to understand the changes in the dynamics when the destruction rate is varied. Although many aspects of the dynamics of Eq. (1) are well understood (see, for example, [18] and references therein), as far as we know, a detailed analysis of the changes in the dynamic behaviour of the solutions of (1) in response to an increasing mortality has not been addressed. In particular, a very important question is if increasing mortality can generate instability; this phenomenon was observed in Mackey's hematological model, but in population dynamics is traditionally assumed that increasing the effort harvesting tends to stabilize the equilibrium [4]. However, we show that this is not always the case, and harvesting can induce sustained oscillations in the Nicholson's blowflies model of population dynamics; this is in agreement with some recent empirical studies that have demonstrated the potential for increasing mortality to lead to instability in plant, insect, and fish populations; see [2,7,40] and references therein.

In one-dimensional discrete population models, the phenomenon of destabilization due to an increasing mortality was explained using the concept of bubbling [22]. For a family of maps $\{f_\lambda\}$ depending smoothly on a parameter $\lambda \in \Lambda$, this means that there

exists an interval $J = (\lambda_1, \lambda_2)$ such that f_λ has a continuous branch of equilibria K_λ satisfying $|f'_\lambda(K_\lambda)| > 1$ for all $\lambda \in (\lambda_1, \lambda_2)$, and $|f'_\lambda(K_\lambda)| < 1$ for all $\lambda \in \Lambda \backslash (\lambda_1, \lambda_2)$. Under some additional assumptions, this situation leads to an structure in the bifurcation diagram as λ is increased which is called *bubble*; this phenomenon was observed in several papers in an ecological context (see [22] for more references). When a bubble exists, the equilibrium typically losses and regains its stability in two period-doubling bifurcations, where $f'_\lambda(K_\lambda) = -1$ (see, e.g., [1,3] for more examples and discussions). As far as we know, in the literature there are not similar studies for continuous population models; even a concept of bubble similar to the one described for discrete models does not seem to have been introduced.

Our main aim in this paper is explaining a similar phenomenon in the framework of delay-differential equations, which will also be referred to as bubbling.

We show that linearization and Hopf bifurcation explain locally the phenomenon of bubbling; in particular, we found the following situation in several examples. For a fixed $\tau > 0$, there is an open interval $I \subset (0, \infty)$ such that:

– equation (1) has a unique positive equilibrium $k(\delta)$ for every $\delta \in I$;
– there exist δ_1, δ_2 in I with $\delta_1 < \delta_2$ so that $\Re\lambda < 0$ holds for all zeros of the characteristic function

$$\lambda + \delta - h'(k(\delta))e^{-\lambda\tau} = 0$$

  associated to the linearized equation of (1) about $k(\delta)$ provided $\delta \in I \backslash (\delta_1, \delta_2)$;
– for $\delta_1 < \delta < \delta_2$ there is at least a complex conjugate pair of zeros of (1) with positive real part.

For the dynamics of equation (1), this means that $k(\delta)$ is locally stable for $\delta \in I \backslash [\delta_1, \delta_2]$, and at δ_1, under additional conditions, $k(\delta)$ loses its stability via a supercritical Hopf bifurcation, where a stable periodic orbit is born, and at δ_2 another supercritical Hopf bifurcation takes place, where a stable periodic orbit disappears. Concerning the global dynamics for $\delta \in I$, we are interested in the consequences of this phenomenon for the long-time behaviour of most solutions of (1). Although this is a too ambitious question, for some particular cases it can be done, as shown in Sect. 2. We give an example for which 0 is globally attractive provided $\delta \in I \backslash [\delta_1, \delta_2]$, and most orbits approach a unique slowly oscillating periodic orbit $\mathcal{O}(\delta)$ for $\delta \in (\delta_1, \delta_2)$. Recall that a periodic solution x of Eq. (1) is called slowly oscillatory if $|t_1 - t_2| > \tau$ for any pair of zeros t_1, t_2 of x. In this case, the subset

$$\bigcup_{\delta \in (\delta_1, \delta_2)} (\delta, \mathcal{O}(\delta))$$

looks like a bubble in $I \times C$, and it plays a dominant role in the global dynamics. Here and throughout the paper, C denotes the Banach space of continuous functions $C([-\tau, 0], \mathbb{R})$ equipped with the maximum norm $|| \cdot ||$.

But for the general case a similar result does not hold. A more modest approach consists of studying where do most solutions go starting from a small neighbourhood of $k(\delta)$ as t tends to infinity, and how the answer depends on δ.

Our results in Sect. 4 imply that for $\delta_1 < \delta < \delta_2$ the slowly oscillatory solutions of (1) leave a neighbourhood of $k(\delta)$. For the case of decreasing h, this means that most solutions of (1) satisfy this property [29,38]. Moreover, we provide an explicit estimate for the size of this neighbourhood, thus proving the existence of bubbling.

When h is unimodal, some numerical results also suggest bubbling phenomena, but in this case the shape of the bubbles seems to be much more complicated.

The paper is organized as follows. In Sect. 2, we present an example for which the global picture of the dynamics is known, and it is easy to describe a bubble. In Sect. 3, we introduce suitable definitions for bubbling in a more general framework. In Sect. 4 we prove two theorems about slowly oscillating periodic solutions. These results can be applied, for Eq. (1) in the above described situation for the linearization, to construct explicit neighbourhoods N_δ, $\delta \in (\delta_1, \delta_2)$, of the unstable stationary point such that there are no slowly oscillatory periodic orbits in N_δ. This fact combined with estimations for the global attractor can give results for the location of bubble-like structures. Section 5 contains upper bounds for bubbles. In Sect. 6 we apply the results in Sects. 4 and 5 to the equations of Mackey and Gurney et al. In particular, some numerical examples are given to explain how an increasing mortality influences the dynamics, depending on the length of the delay parameter τ. We include a comparison with the limiting difference equation formally obtained as $\tau \to \infty$ in (1).

This paper is only the first attempt to understand bubbling for delay differential equations. Rigorous proofs are not available for most of the numerically observed phenomena. There are many open problems even for simple looking nonlinearities.

2 An Example

In this section, we show an example for the existence of a bubble. Consider

$$x'(t) = -\delta x(t) - b\beta(\delta) \arctan(x(t-1)), \tag{2}$$

where $\delta > 0$, $b > 0$, and a smooth function $\beta : (0, \infty) \to (0, \infty)$ will be specified later. It is easy to check that the unique equilibrium is $x = 0$. The linearized equation of (2) about 0 is

$$y'(t) = -\delta y(t) - \alpha y(t-1) \tag{3}$$

with $\alpha = b\beta(\delta)$.

The characteristic equation is

$$\lambda + \alpha e^{-\lambda} + \delta = 0. \tag{4}$$

Equation (4) is well studied (see [8, Chapter XI]). It is known that the border of asymptotic stability is given by the curve implicitly defined by

$$\arccos\left(\frac{-\delta}{\alpha}\right) = \sqrt{\alpha^2 - \delta^2}.$$

Fig. 1 The *solid lines* represent the values of $(\alpha, \delta) \in (0, 4) \times (0, 10)$ for which the first and second branches of eigenvalues of Eq. (3) cross the imaginary axis. The equilibrium is asymptotically stable below the *lower solid line*; otherwise, it is unstable. The *numbers* between the curves indicate how many roots the characteristic equation has with positive real part. The *dashed line* is the graph of $\alpha(\delta) = 7\beta(\delta) = 7\delta^2 e^{-\delta}$
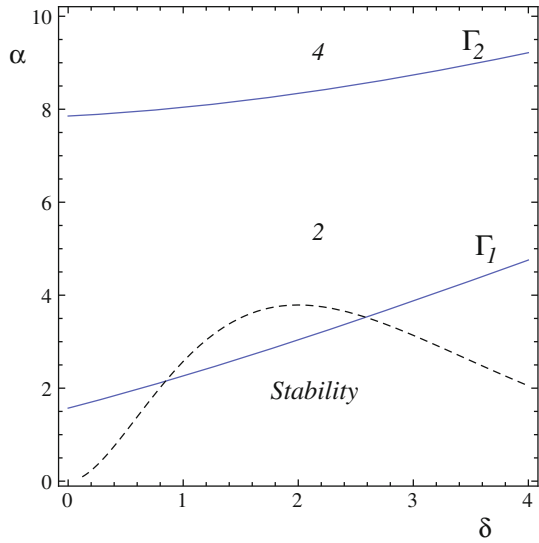
This curve is determined by the values of (α, δ) in $(0, \infty) \times (0, \infty)$ for which the first branch of eigenvalues of (3) crosses the imaginary axis. It is represented by the lower solid line in Fig. 1, for $\delta \in (0, 4)$ and $\alpha \in (0, 10)$. The equilibrium of Eq. (2) is asymptotically stable for the values (δ, α) below this curve. The points (δ, α) for which the second branch of eigenvalues crosses the imaginary axis is defined by

$$\arccos\left(\frac{-\delta}{\alpha}\right) + 2\pi = \sqrt{\alpha^2 - \delta^2}.$$

Such a curve is the upper solid line in Fig. 1. Between this pair of curves, Eq. (4) has exactly two eigenvalues with positive real part.

An application of the implicit function theorem gives that there are C^1-smooth functions $\gamma_i : (0, \infty) \to (0, \infty), i \in \{1, 2\}$, such that the above two curves have the graph representations

$$\Gamma_i = \{(\delta, \gamma_i(\delta)) : \delta > 0\}, \quad (i \in \{1, 2\}),$$

respectively. In addition, $\gamma_2(\delta) > \gamma_1(\delta) > 0$ for all $\delta > 0$, and $\gamma_1(\delta) \to \pi/2$ as $\delta \to 0+$. Then it is an elementary exercise to construct a smooth function $\beta : (0, \infty) \to (0, \infty)$ such that, for a range of values of b, the graphs of $b\beta$ and γ_1 have exactly two intersections at some δ_1, δ_2 with $\delta_1 < \delta_2$, and $b\beta$ has no intersection with γ_2. With this choice of β, clearly, $b\beta(\delta) < \gamma_1(\delta)$ for all $\delta \in (0, \delta_1) \cup (\delta_2, \infty)$, and $b\beta(\delta) > \gamma_1(\delta)$ for all $\delta \in (\delta_1, \delta_2)$.

Recent results of the first author [17,18] show that the equilibrium of (2) is globally asymptotically stable whenever it is locally asymptotically stable, i.e., for $\delta \in (0, \delta_1) \cup (\delta_2, \infty)$, and, for $\delta \in (\delta_1, \delta_2)$, (2) has exactly one periodic solution (up to time translation) which is slowly oscillating. The periodic orbit defined by this
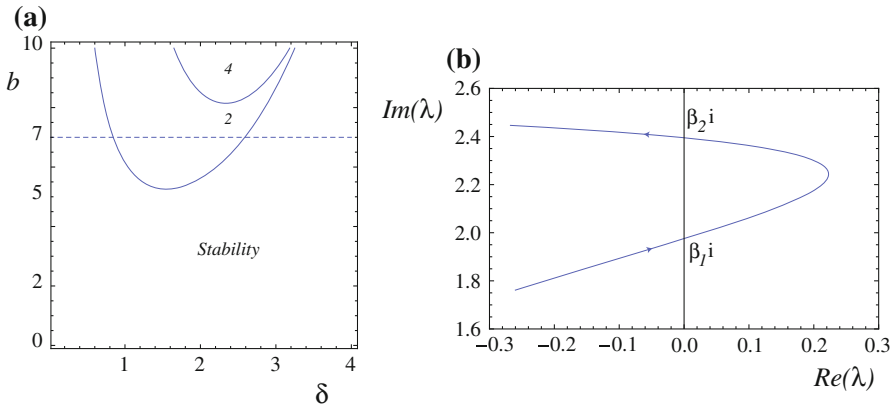
(a)

(b)

Fig. 2 **a** Stability chart of Eq. (2) with $\beta(\delta) = \delta^2 e^{-\delta}$, $\delta \in (0, 4)$ and $b \in (0, 10)$. **b** First branch of eigenvalues in the complex plane for $b = 7$ and $\delta \in (0.6, 3.2)$

slowly oscillating periodic solution attracts all points of the phase space C except the equilibrium.

If an intersection of β and γ_2 is allowed in (δ_1, δ_2) then there is still a unique slowly oscillating periodic orbit, and more (rapidly oscillating) periodic orbits may appear. However, the unique slowly oscillatory periodic orbit attracts all points of an open and dense subset of the phase C, see [29].

Choose $\beta(\delta) = \delta^2 e^{-\delta}$. The dashed curve in Fig. 1 is the graph of $7\beta(\delta)$, which meets the requirements stated above.

In Fig. 2a, we represent the stability chart of Eq. (2) in the plane (δ, b), with $\beta(\delta) = \delta^2 e^{-\delta}$, $\delta \in (0, 4)$ and $b \in (0, 10)$. The lower curve represents the boundary of the asymptotic stability region of the equilibrium of (2), and it is defined by the implicit equation

$$\arccos\left(\frac{-\delta}{b\beta(\delta)}\right) = \sqrt{b^2(\beta(\delta))^2 - \delta^2},$$

that is,

$$\arccos\left(\frac{-e^\delta}{b\delta}\right) = \delta\sqrt{b^2\delta^2 e^{-\delta} - 1}.$$

For $b = 7$, there are two intersections $(\delta_1, 7)$, $(\delta_2, 7)$ with this curve, and empty intersection with the second curve, defined by

$$\arccos\left(\frac{-e^\delta}{b\delta}\right) + 2\pi = \delta\sqrt{b^2\delta^2 e^{-\delta} - 1}.$$

We show in Fig. 2b a parametric representation of the first branch of roots $\lambda(\delta)$ of (4), with $\alpha = 7\delta^2 e^{-\delta}$, in the complex plane for $\delta \in (0.6, 3.2)$ (only the roots with

Fig. 3 Representation of a bubble in Eq. (5) as δ is increased. For each δ, the amplitude of the attracting periodic solution is shown
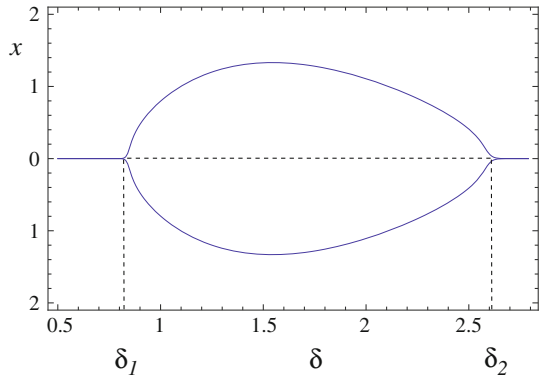
positive real part are plotted). The arrows show the direction of increasing δ. The equilibrium loses its asymptotic stability in a supercritical Hopf bifurcation at $\delta_1 \approx 0.845$, and becomes stable again after a second Hopf bifurcation occurs at $\delta_2 \approx 2.587$. The values of $\beta_1 i \approx 1.975i$, $\beta_2 i \approx 2.395i$ for which the curve crosses the imaginary axis can be obtained by the formula

$$\beta_k = \sqrt{\alpha^2 - \delta_k^2} = \delta_k \sqrt{49\delta_k^2 e^{-2\delta_k} - 1}, \quad k = 1, 2.$$

In Fig. 3, we show a numerical bifurcation diagram for equation

$$x'(t) = -\delta x(t) - 7\delta^2 e^{-\delta} \arctan(x(t-1)) \tag{5}$$

as δ is increased. A "bubble" appears as we plot the minimum and the maximum reached by the periodic solutions between the two Hopf bifurcation points (so it gives an approximation of the amplitudes of the periodic solutions); the unstable equilibrium between the two Hopf bifurcation points is indicated by a dashed line. A formal definition of bubble is given in the next section.

3 Definition of Bubbles

In this section we give a formal definition of the bubbling phenomenon and bubbles in a class of delay differential equations more general than (1). We recall that for $\tau > 0$, we denote by C the Banach space $C([-\tau, 0], \mathbb{R})$ equipped with the maximum norm $\| \cdot \|$. For a continuous map $u : J \to \mathbb{R}$ defined on an interval J, and for $t \in J$ with $t - \tau \in J$, define $u_t \in C$ by $u_t(s) = u(t+s)$, $-\tau \le s \le 0$.

Consider the delay-differential equation

$$x'(t) = f(\delta, x_t) \tag{6}$$

for parameter values δ in an open interval $I \subset (0, \infty)$. Let an open set $U \subset I \times C$ be given so that $I \times \{(0)\} \subset U$. Suppose that $f : U \to \mathbb{R}$ is continuously differentiable, and $f^{-1}(0) = \{(\delta, 0) \in U : \delta \in I\}$. For $\delta \in I$, define $U_\delta = \{\phi \in C : (\delta, \phi) \in U\}$.

We assume that for all $\delta \in I$ every $\phi \in U_\delta$ uniquely determines a solution $x = x^\phi : [-\tau, \infty) \to \mathbb{R}$ of (6), i.e., a continuous function $x : [-\tau, \infty) \to \mathbb{R}$ such that x is differentiable on $(0, \infty)$, $x_0 = \phi$, and x satisfies (6) with δ for all $t > 0$. Then the solutions of Eq. (6) generate the semiflow

$$F_\delta : [0, \infty) \times U_\delta \ni (t, \phi) \mapsto x_t^\phi \in U_\delta$$

for all $\delta \in I$. We have $F_\delta(t, 0) = 0$, $t \geq 0$, and 0 is the only stationary point.

Remark 1 We notice that Eq. (1) fits to this setting in the most usual examples. Indeed, assume $h : [0, \infty) \to \mathbb{R}$ is a smooth function with $h((0, \infty)) \subset (0, \infty)$. In addition, suppose that, for parameters $\delta > 0$ in an interval I, the map $(0, \infty) \ni \xi \mapsto -\delta\xi + h(\xi) \in \mathbb{R}$ has a unique zero denoted by $k(\delta)$. Then for positive solutions x via the transformation $y = x - k(\delta)$ we get the equivalent equation

$$y'(t) = -\delta y(t) + h(y(t - \tau) + k(\delta)) - h(k(\delta)) \tag{7}$$

for $\delta \in I$. With $f(\delta, \phi) = -\delta\phi(0) + h(k(\delta) + \phi(-\tau)) - h(k(\delta))$ and

$$U = \{(\delta, \phi) \in I \times C : \delta \in I, \quad \min_{s \in [-\tau, 0]} \phi(s) + k(\delta) > 0\},$$

equation (1) will be of the form of (6).

The derivatives $D_2 F_\delta(t, 0)$, $t \geq 0$, form a strongly continuous semigroup, and $D_2 F_\delta(t, 0)\psi = v_t^\psi$ where v^ψ is the solution of the linear variational equation

$$v'(t) = D_2 f(\delta, 0)v_t \tag{8}$$

with $v_0^\psi = \psi \in C$, and D_2 denotes the partial derivative with respect to the second variable. The linearization of Eq. (7) at 0 gives the characteristic function

$$\mathbb{C} \ni \lambda \mapsto \lambda - D_2 f(\delta, 0)e^{\lambda \cdot} \in \mathbb{C} \tag{9}$$

where $e^{\lambda \cdot} \in C([-\tau, 0], \mathbb{C})$ is given by $e^{\lambda \cdot}(s) = e^{\lambda s}$, $s \in [-\tau, 0]$. The location of zeros of (9) gives information about the dynamics near the stationary point 0. As it was shown for Eq. (2), for fixed $\tau > 0$, the number of zeros of characteristic function (9) as a function of δ in the set $\{\lambda \in \mathbb{C} : \Re\lambda > 0\}$ may change in a nonmonotone way due to the δ-dependence of the term $D_2 f(\delta, 0)$.

We assume that for all $\delta \in I$ the semiflow F_δ has a global attractor $\mathcal{A}(\delta)$, that is a nonempty, compact, invariant subset of U_δ so that $\mathcal{A}(\delta)$ attracts all bounded subsets of U_δ. We refer to [14] for sufficient conditions for the existence of global attractors. Under this condition, for $\delta \in I$ and $\phi \in U_\delta$ the ω-limit set $\omega_\delta(\phi)$ of ϕ exists, and it is a nonempty, compact, invariant subset of $\mathcal{A}(\delta)$.

Such concepts as equilibrium, periodic orbit, attractor, invariant set, and bifurcations are introduced in a natural way; for precise definitions, we refer to the classical monograph of Hale and Lunel [15], or the recent book of Smith [35].

For a set $S \subset C$ the distance of 0 from S is defined by $\text{dist}(0, S) = \inf_{\phi \in S} ||\phi||$. Let $\text{cl}(S)$ denote the closure of S in C. For $r > 0$ set $C_r = \{\phi \in C : ||\phi|| < r\}$.

We will use the following hypothesis on the characteristic function (9).

(H)   There exist δ_1, δ_2 in I with $\delta_1 < \delta_2$ so that, for all $\delta \in I \backslash [\delta_1, \delta_2]$, all zeros λ of the characteristic Eq. (9) satisfy $\Re\lambda < 0$, and, for $\delta_1 < \delta < \delta_2$, the characteristic function (9) has at least one pair of complex conjugate zeros $\lambda_0, \overline{\lambda_0}$ with $\Re\lambda_0 > 0$ and $\Im\lambda_0 \neq 0$.

Definition 1 We say that Eq. (6) exhibits bubbling if **(H)** holds and for all $\delta \in (\delta_1, \delta_2)$ there exist $r_\delta > 0$ and an open and dense subset V_δ of C_{r_δ} such that

$$\inf_{\phi \in V_\delta} \text{dist}(0, \omega_\delta(\phi)) > 0.$$

In this case the set

$$\mathcal{B} = \bigcup_{\delta_1 < \delta < \delta_2} \left(\delta, \bigcap_{r>0} \text{cl} \left(\bigcup_{\phi \in V_\delta \cap C_r} \omega_\delta(\phi) \right) \right)$$

is called a bubble.

Notice that if a bubble exists for Eq. (6) then, for any $r > 0$ and $\delta \in (\delta_1, \delta_2)$, the set

$$\text{cl} \left(\bigcup_{\phi \in V_\delta \cap C_r} \omega_\delta(\phi) \right)$$

is a nonempty and closed subset of the global attractor $\mathcal{A}(\delta)$, and its distance from 0 is positive. Then the set

$$\bigcap_{r>0} \text{cl} \left(\bigcup_{\phi \in V_\delta \cap C_r} \omega_\delta(\phi) \right)$$

is nonempty with a positive distance from 0.

From the discussion in the previous section, we can ensure that Eq. (5) has a bubble as δ is increased. In fact in this case, according to Definition 1, the bubble $\mathcal{B}$ is given by

$$\mathcal{B} = \bigcup_{\delta \in (\delta_1, \delta_2)} (\delta, \mathcal{O}(\delta))$$

where $\mathcal{O}(\delta)$ denotes the unique periodic orbit. See Fig. 3 for a graphic representation of $\mathcal{B}$.

4 Location of Slowly Oscillating Periodic Orbits

We recall that a solution $x : J \to \mathbb{R}$, defined on an interval J, of the delay-differential equation (6) will be called slowly oscillatory if $|z_1 - z_2| > \tau$ holds for each pair of zeros z_1, z_2 of x.

In this section we assume the unstable situation of hypothesis **(H)** for an equation and first prove the nonexistence of slowly oscillating periodic solutions in a neighbourhood of 0. Then we estimate the distance of slowly oscillating periodic orbits from 0. This information can be applied to show the existence of bubbles provided slow oscillation dominates the dynamics. In particular this is the case for Eq. (1) when h is monotone decreasing due to the results of Mallet-Paret and Walther [29] (see also [18,38]). The result below is an extension of [37].

Assume that $a > 0, A > 0, B > 0, J \subset \mathbb{R}$ is an open interval with $[-A, B] \subset J$, and $g : J \to \mathbb{R}$ is a C^1-smooth function with $g(0) = 0$ and $g'(\xi) > 0$ for all $\xi \in [-A, B]$. There is a unique $\omega \in (\pi/2, \pi)$ with $\omega = -a \tan \omega$. Set $b = \sqrt{a^2 + \omega^2}$. Consider the equations

$$x'(t) = -ax(t) - g(x(t - 1)) \tag{10}$$

and

$$y'(t) = -ay(t) - by(t - 1). \tag{11}$$

Clearly, for all $k \in \mathbb{R} \backslash \{0\}$ and $\tau \in \mathbb{R}$ the function $y(t) = k \sin(\omega t + \tau), t \in \mathbb{R}$, is a periodic solution of Eq. (11) with minimal period $2\pi/\omega \in (2, 4)$.

Theorem 1 *If*

$$g'(\xi) > b \quad for \ all \ \xi \in [-A, B] \tag{12}$$

then Eq. (10) has no slowly oscillatory periodic solution x with $x(\mathbb{R}) \subset [-A, B]$.

Proof Suppose that x is a slowly oscillatory periodic solution of (10) with $x(\mathbb{R}) \subset [-A, B]$. From [28] we know that if $T > 0$ is the minimal period of x, then there are t_0, t_1 in $\mathbb{R}$ so that $x(t_0) = \min_{t \in \mathbb{R}} x(t), t_0 < t_1 < t_0 + T, x(t_1) = \max_{t \in \mathbb{R}} x(t), x'(t) > 0$ for all $t \in (t_0, t_1), x'(t) < 0$ for all $t \in (t_1, t_0 + T)$, moreover $t_1 - t_0 > 1, t_0 + T - t_1 > 1$.

It follows that the image of

$$X : [0, T] \ni t \mapsto (x(t), x'(t)) \in \mathbb{R}^2$$

is a simple closed curve with $(0, 0)$ in its interior. We denote by $|X| = X([0, T])$ the trace of X. Recall that by the Jordan curve theorem $\mathbb{R}^2 \backslash |X|$ consists of exactly two connected components, one bounded and the other unbounded; we denote them by $\text{int}(X)$ and $\text{ext}(X)$, respectively.

For $k > 0$ define the curves

$$Y_k : \left[0, \frac{2\pi}{\omega}\right] \ni t \mapsto k(\sin(\omega t), \omega \cos(\omega t)) \in \mathbb{R}^2.$$

Clearly, the trace $|Y_k|$ of Y_k is the ellipse $\{(u, v) \in \mathbb{R}^2 : u^2 + v^2/\omega^2 = k^2\}$.
There exists $k_0 > 0$ so that

$$|X| \subset \text{ext}(Y_k) \quad \text{for all } k \in (0, k_0)$$

and

$$|X| \cap |Y_{k_0}| \neq \emptyset.$$

Then

$$|X| \subset \text{ext}(Y_{k_0}) \cup |Y_{k_0}| \tag{13}$$

follows. Set $z(t) = k_0 \sin(\omega t), t \in \mathbb{R}$, and $Z = Y_{k_0}$.
  By the definition of k_0, there are t_*, t_{**} in $\mathbb{R}$ such that $X(t_*) = Z(t_{**}) \in |X| \cap |Z|$.
Replacing $x(\cdot)$ by $x(\cdot + t_*)$ and $z(\cdot)$ by $z(\cdot + t_{**})$, we may assume $t_* = t_{**} = 0$, i.e.,

$$x(0) = z(0), \quad x'(0) = z'(0).$$

  Suppose $x'(0) = z'(0) = 0$. The fact $(0, 0) \notin |X| \cup |Z|$ gives $x(0) = z(0) = c \neq 0$.
We consider only the case $c > 0$ as the case $c < 0$ is analogous. Clearly, $c = k_0$. From
the above properties of the slowly oscillatory periodic solutions x and z,

$$x'(s) > 0, \; z'(s) > 0 \quad \text{for all } s \in [-1, 0).$$

Equations (10), (11) and $x'(0) = z'(0) = 0, x(0) = z(0) = k_0 > 0$ combined yield

$$g(x(-1)) = -ax(0) = -az(0) = bz(-1) < 0 \quad \text{and} \quad x(-1) < 0, \; z(-1) < 0.$$

By the mean value theorem, $g(x(-1)) = g'(\xi)x(-1)$ for some $\xi \in (x(-1), 0)$.
Applying (12),

$$z(-1) < x(-1) < 0 \tag{14}$$

follows.
  Let

$$\tau_x : [x(-1), c] \to [-1, 0], \quad \tau_z : [z(-1), c] \to [-1, 0]$$

denote the inverses of $x|_{[-1,0]}, z|_{[-1,0]}$, respectively. The functions

$$\phi_x : [x(-1), c] \ni u \mapsto x'(\tau_x(u)) \in \mathbb{R}, \; \phi_z : [z(-1), c] \ni u \mapsto z'(\tau_z(u)) \in \mathbb{R}$$

satisfy $\phi_x(c) = \phi_z(c) = 0$, and $\phi_x(u) > 0$ for all $u \in [x(-1), c)$, $\phi_z(u) > 0$ for all $u \in [z(-1), c)$. The arcs

$$\Omega_x = \{X(t) : t \in [-1, 0]\} \quad \text{and} \quad \Omega_z = \{Z(t) : t \in [-1, 0]\}$$

coincide with the graphs

$$\{(u, \phi_x(u)) : u \in [x(-1), c]\} \quad \text{and} \quad \{(u, \phi_z(u)) : u \in [z(-1), c]\},$$

respectively. The inclusion (13) and inequality (14) imply

$$0 < \phi_z(u) \le \phi_x(u) \quad \text{for all } u \in [x(-1), c). \tag{15}$$

The equation $x'(s) = \phi_x(x(s))$, $s \in [-1, 0]$, and $x'(s) > 0$ for $s \in [-1, 0)$ combined yield

$$1 = \lim_{\epsilon \to 0+} (1 - \epsilon) = \lim_{\epsilon \to 0+} \int_{-1}^{-\epsilon} \frac{x'(s)}{\phi_x(x(s))} \, ds = \int_{x(-1)}^{c} \frac{du}{\phi_x(u)}$$

where the last integral is improper. Similarly,

$$1 = \int_{z(-1)}^{c} \frac{du}{\phi_z(u)}.$$

Consequently,

$$\int_{x(-1)}^{c} \frac{du}{\phi_x(u)} = \int_{z(-1)}^{c} \frac{du}{\phi_z(u)}.$$

This is impossible by (14), (15) and $\phi_z(u) > 0$ for $u \in [z(-1), c)$. Therefore, $x'(0) = z'(0) \ne 0$.

We have $x'(0) = z'(0) \ne 0$. Set $d = x(0) = z(0)$. By continuity, x and z have inverses in small t-intervals containing 0. Choose a sufficiently small $\delta > 0$ so that

$$t_x : (d - \delta, d + \delta) \to \mathbb{R} \quad \text{and} \quad t_z : (d - \delta, d + \delta) \to \mathbb{R}$$

are the inverses of restrictions of x and z to some open intervals around 0, respectively, and $x'(t_x(u)) \ne 0$, $z'(t_z(u)) \ne 0$ for all $u \in (d - \delta, d + \delta)$. Setting

$$\eta_x : (d - \delta, d + \delta) \ni u \mapsto x'(t_x(u)) \in \mathbb{R}, \ \eta_z : (d - \delta, d + \delta) \ni u \mapsto z'(t_z(u)) \in \mathbb{R},$$

the sets

$$\{(u, \eta_x(u)) : u \in (d - \delta, d + \delta)\}, \ \{(u, \eta_z(u)) : u \in (d - \delta, d + \delta)\}$$

are graph representations of the restrictions $X|_I$, $Z|_J$ to the open intervals $I = t_x((d - \delta, d + \delta))$, $J = t_z((d - \delta, d + \delta))$, respectively. Applying $|X| \subset |Z| \cup \text{ext}(Z)$, $\eta_x(d) = \eta_z(d)$, and the C^1-smoothness of η_x and η_z, it follows that

$$\eta_x'(d) = \eta_z'(d).$$

We have

$$\eta_x'(u) = \frac{x''(t_x(u))}{x'(t_x(u))}, \quad \eta_z'(u) = \frac{z''(t_z(u))}{z'(t_z(u))}.$$

Consequently, by $t_x(d) = 0 = t_z(d)$,

$$\frac{x''(0)}{x'(0)} = \frac{z''(0)}{z'(0)}.$$

Hence, by $x'(0) = z'(0)$, one gets $x''(0) = z''(0)$.

Consequently, using (10), (11) and their derivatives at $t = 0$, we obtain

$$g'(x(-1))x'(-1) = bz'(-1) \tag{16}$$

and

$$g(x(-1)) = bz(-1). \tag{17}$$

Assume $x(-1) = 0$ or $z(-1) = 0$. From (17), $x(-1) = z(-1) = 0$ follows. Then $x'(-1) \neq 0$, $z'(-1) \neq 0$ since both x and z are slowly oscillating periodic solutions of (10) and (11), respectively. From $g'(0) > b$ and (16), either

$$0 < x'(-1) < z'(-1)$$

or

$$z'(-1) < x'(-1) < 0.$$

In either case, $X(-1) \in \text{int}(Z)$, a contradiction. This shows $x(-1) \neq 0$ and $z(-1) \neq 0$.

If $x'(-1) = 0$ or $z'(-1) = 0$, then, by (16), $x'(-1) = z'(-1) = 0$. Hence $x(-1) \neq 0$, $z(-1) \neq 0$, and by (12) and (17), either

$$0 < x(-1) < z(-1)$$

or

$$z(-1) < x(-1) < 0.$$

In both cases, $X(-1) \in \text{int}(Z)$, a contradiction. Thus, $x'(-1) \neq 0$, $z'(-1) \neq 0$.

Therefore, $x(-1) \neq 0$, $z(-1) \neq 0$, and $x'(-1) \neq 0$, $z'(-1) \neq 0$. Equalities (16), (17), and condition (12) on g imply one of the following cases:

$$0 < x(-1) < z(-1), \ 0 < x'(-1) < z'(-1);$$
$$0 < x(-1) < z(-1), \ z'(-1) < x'(-1) < 0;$$
$$z(-1) < x(-1) < 0, \ 0 < x'(-1) < z'(-1);$$
$$z(-1) < x(-1) < 0, \ z'(-1) < x'(-1) < 0.$$

In each case $X(-1) \in \text{int}(Z)$ holds, a contradiction. This completes the proof. $\square$

Let a, b, A, B, g be given as before. Suppose that the C^1-smooth map $g : J \to \mathbb{R}$ is defined on the larger interval J instead of $(-A, B)$, and g satisfies condition (12) and

$$\xi g(\xi) > 0 \quad \text{for all } \xi \in J \setminus \{0\}. \tag{18}$$

Denoting the inverse of $g|_{[-A,B]}$ by g^{-1}, we define $G : \mathbb{R} \to \mathbb{R}$ by

$$G(u) = \begin{cases} -A & \text{if } u < g(-A) \\ g^{-1}(u) & \text{if } g(-A) \leq u \leq g(B) \\ B & \text{if } u > g(B) \end{cases}$$

Set

$$g_- : [0, A] \ni u \mapsto u - g(-u) \in \mathbb{R}, \quad g_+ : [0, B] \ni u \mapsto u + g(u) \in \mathbb{R}.$$

Clearly, g_- and g_+ are injective, and $g_-([0, A]) = [0, A - g(-A)]$, $g_+([0, B]) = [0, B + g(B)]$. Let g_-^{-1} and g_+^{-1} denote the inverses. Define

$$G_-(u) = \begin{cases} g_-^{-1}(u) & \text{if } 0 \leq u \leq A - g(-A) \\ A & \text{if } u > A - g(-A) \end{cases}$$

and

$$G_+(u) = \begin{cases} g_+^{-1}(u) & \text{if } 0 \leq u \leq B + g(B) \\ B & \text{if } u > B + g(B). \end{cases}$$

Theorem 2 *Assume the above conditions on a, b, A, B and $g : J \to \mathbb{R}$. Let x be a slowly oscillatory periodic solution of Eq. (10) with*

$$\min_{t \in \mathbb{R}} x(t) = -m, \quad \max_{t \in \mathbb{R}} x(t) = M.$$

Then $-m \leq G(-B)$, $M \geq G(A)$, *and*

$$||x_t|| \geq \min \{G_-(G(A)), G_+(-G(-B))\} \quad \textit{for all } t \in \mathbb{R}.$$

Proof As x is a slowly oscillatory periodic solution, there exist zeros z_0, z_1, z_2 of x with $z_0 + 1 < z_1, z_1 + 1 < z_2, x(t) < 0$ for $t \in (z_0, z_1)$, $x(t) > 0$ for $t \in (z_1, z_2)$, and the minimal period of x is $z_2 - z_0$. These facts, the negative feedback condition (18) and Eq. (10) combined yield that $x'(t) > 0$ for all $t \in [z_0 + 1, z_1]$ and $x'(t) < 0$ for all $t \in [z_1 + 1, z_2]$. Consequently, there exist $t_1 \in (z_1, z_1 + 1)$ and $t_2 \in (z_2, z_2 + 1)$ such that $x(t_1) = M$ and $x(t_2) = -m$.

As $G(\mathbb{R}) = [-A, B]$, obviously $G(-B) \geq -A$ and $G(A) \leq B$. Thus, the statement clearly holds for m and M provided $-m \leq -A$ and $M \geq B$, respectively.

We distinguish two cases according as $M \geq B$ or $M < B$.

Case 1 $M \geq B$. If $-m \leq -A$ then there is nothing to prove. Assume $-A < -m < 0$. Integrating equation (10) on $[z_1, t_1]$, using that $x(\mathbb{R}) = [-m, M] \subset (-A, \infty)$ implies $-g(x(t)) \leq -g(-m)$ for all $t \in \mathbb{R}$, and $t_1 - z_1 < 1$, we obtain

$$\begin{aligned} B \leq M &= x(t_1) - x(z_1) = \int_{z_1}^{t_1} x'(t)\, dt = \int_{z_1}^{t_1} [-ax(t) - g(x(t-1))]\, dt \\ &< \int_{z_1-1}^{t_1-1} [-g(x(t))]\, dt < -g(-m)(t_1 - z_1) \\ &< -g(-m). \end{aligned}$$

Consequently, $-B \in (g(-m), 0) \subset (g(-A), 0)$, and $-m \leq g^{-1}(-B) = G(-B)$.

Case 2 $M < B$. Then $-m < -A$ by Theorem 1. There exists $t_2 \in (z_2, z_2 + 1)$ with $x(t_2) = -m$. Integrating equation (10) on $[z_2, t_2]$, using that $x(\mathbb{R}) = [-m, M] \subset (-\infty, B)$ implies $-g(x(t)) \geq -g(M)$ for all $t \in \mathbb{R}$, and $t_2 - z_2 < 1$, we obtain

$$\begin{aligned} -A > -m &= x(t_2) - x(z_2) = \int_{z_2}^{t_2} x'(t)\, dt = \int_{z_2}^{t_2} [-ax(t) - g(x(t-1))]\, dt \\ &> \int_{z_2-1}^{t_2-1} [-g(x(t))]\, dt > -g(M)(t_2 - z_2) \\ &> -g(M), \end{aligned}$$

that is $g(M) > A$. Hence $M > g^{-1}(A) = G(A)$ follows.

Now we prove the lower bound for $\min_{t \in \mathbb{R}} ||x_t||$. The properties of x mentioned at the beginning of the proof clearly imply that

$$\begin{aligned} ||x_s|| &\geq ||x_{z_1}|| && \text{for all } s \in [z_0 + 1, z_1], \\ ||x_s|| &\geq ||x_{z_2}|| && \text{for all } s \in [z_1 + 1, z_2], \\ ||x_s|| &\geq ||x_{z_1+1}|| \geq ||x_{z_2}|| && \text{for all } s \in [t_1, z_1 + 1], \\ ||x_s|| &\geq ||x_{z_2+1}|| \geq ||x_{z_1}|| && \text{for all } s \in [t_2, z_2 + 1]. \end{aligned}$$

Then

$$||x_t|| \geq \min_{s \in [z_1, t_1] \cup [z_2, t_2]} ||x_s||$$

follows for all $t \in \mathbb{R}$.

Let $s \in [z_1, t_1]$ and assume that $||x_s|| = \beta$. If $\beta \geq A$ then trivially $\beta \geq G_-(G(A))$ since $G_-([0, \infty)) = [0, A]$. So, suppose $0 < \beta < A$. Then $0 \leq x(s) \leq \beta$. Integrating equation (10) on $[s, t_1]$ we get

$$M - \beta \leq M - x(s) = x(t_1) - x(s) = \int_s^{t_1} x'(t)\, dt = \int_s^{t_1}[-ax(t) - g(x(t-1))]\, dt$$
$$< \int_{s-1}^{t_1-1}[-g(x(t))]\, dt$$
$$< -g(-\beta).$$

Hence

$$G(A) \leq M < \beta - g(-\beta) = g_-(\beta)$$

and $\beta > G_-(G(A))$ follows.

Analogously, let $s \in [z_2, t_2]$ and $||x_s|| = \gamma$. We may assume $0 < \gamma < B$ since the statement is obvious in case $\beta \geq B$. Then $-\gamma \leq x(s) \leq 0$. Integrating equation (10) on $[s, t_2]$ we obtain

$$-m + \gamma \geq -m - x(s) = x(t_2) - x(s) = \int_s^{t_2} x'(t)\, dt = \int_s^{t_2}[-ax(t) - g(x(t-1))]\, dt$$
$$> \int_{s-1}^{t_2-1}[-g(x(t))]\, dt$$
$$> -g(\gamma).$$

Hence

$$g_+(\gamma) = \gamma + g(\gamma) > m \geq -G(-B)$$

and $\gamma > G_+(-G(-B))$ follows. This completes the proof. $\qquad\qquad\square$

Theorem 2 provides a neighbourhood of $0 \in C$ where periodic orbits corresponding to slowly oscillating periodic solutions cannot enter.

As an illustration, we apply it to Eq. (5). In this case

$$g(x) = 7\delta^2 e^{-\delta} \arctan(x); \quad g'(x) = \frac{7\delta^2 e^{-\delta}}{1 + x^2} > 0.$$

To use Theorem 2, notice that

$$g'(x) > b \iff \frac{7\delta^2 e^{-\delta}}{1 + x^2} > b \iff |x| < \left(\frac{7\delta^2 e^{-\delta}}{b} - 1\right)^{1/2}.$$

Thus we can define

$$A(\delta) = B(\delta) = \left(\frac{7\delta^2 e^{-\delta}}{b} - 1\right)^{1/2}, \tag{19}$$

where $b = (\delta^2 + \omega^2)^{1/2}$, and ω is the unique solution of $\omega = -\delta \tan(\omega)$ in $(\pi/2, \pi)$.

Fig. 4 The *inner curve* (constructed using Theorem 2) delimits the neighbourhood of 0 free of slowly oscillatory periodic orbits of Eq. (5) for the values of δ between the two Hopf bifurcation points. The *exterior curve* is obtained integrating numerically the equation and plotting the minimum norm of the points of the periodic orbit in the phase space
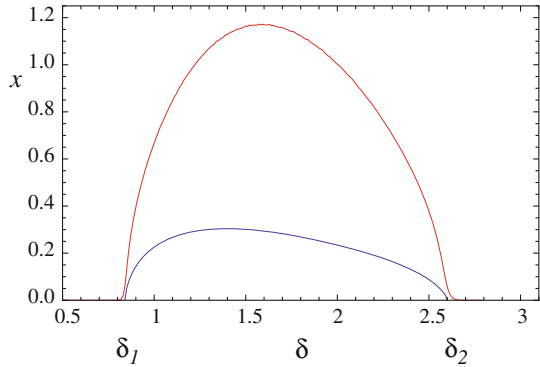
The parametric curve

$$\left(\delta, \min\left\{G_-^*(G(A(\delta))), G_+^*(-G(-B(\delta)))\right\}\right)$$

for $\delta \in (\delta_1, \delta_2) \approx (0.845, 2.587)$ provides the inner curve in Fig. 4. The exterior curve is a numerical approximation obtained integrating numerically the equation and plotting the minimum of the norms of the segments x_t over a period.

5 Upper Bounds for Bubbles

Theorems 1 and 2 allow us to find a neighborhood of zero free of slowly oscillatory periodic solutions, giving in this way a lower bound for the distance of bubbles to zero, at least in some cases. In this section, we provide some upper bounds for the location of bubbles. For it, we use some results based on attracting invariant intervals for an auxiliary one-dimensional discrete equation [13,20,21]. The results below, together with those proved in Sect. 4, enable us to represent a bounded and bounded away from zero region in which the maximum and the minimum of the periodic solutions should be; such results will be applied to validate the numerical experiments made for Eq. (5), for the Mackey equation, and for the Nicholson's blowflies equation.

Consider the equation

$$x'(t) = -ax(t) - g(x(t-1)), \tag{20}$$

where $g : I \to I$ is a continuously differentiable function defined on an open real interval I, with $0 \in I$. We assume that $g(x) = x$ if and only if $x = 0$. Define the auxiliary map

$$h_a(x) := \frac{e^{-a} - 1}{a} g(x).$$

In case g is a unimodal map, we can apply the following result, which is a slight modification of [20, Corollary 9]:

Proposition 1 *Assume that there exists $c < 0$ such that $h'_a(x) > 0$ for all $x < c$, and $h'_a(x) < 0$ for all $x > c$. Then the map h_a has a globally attracting invariant set $[\alpha, \beta] = [h_a(h_a(c)), h_a(c)]$. Moreover, for every solution $x(t)$ of (20) the following inequalities hold:*

$$\alpha \leq \liminf_{t \to \infty} x(t) \leq \limsup_{t \to \infty} x(t) \leq \beta.$$

If g is strictly decreasing and bounded either from below or from above, then the map h_a also has a globally attracting invariant set, and a result similar to Proposition 1 holds. If some additional conditions are assumed, this invariant set can be considerably shrunken. We recall that the Schwarzian derivative of a C^3 map f is defined by the relation

$$(Sf)(x) = \frac{f'''(x)}{f'(x)} - \frac{3}{2}\left(\frac{f''(x)}{f'(x)}\right)^2,$$

whenever $f'(x) \neq 0$.

For decreasing maps with negative Schwarzian derivative, we can apply the following dichotomy result which follows from [21, Proposition 5]:

Proposition 2 *Assume that h_a has a globally attracting invariant set $[\alpha, \beta]$, and $h'_a(x) < 0$, $(Sh_a)(x) < 0$ for all $x \in [\alpha, \beta]$, where Sh_a is the Schwarzian derivative of h_a.*

(a) *If $-1 \leq h'_a(0) < 0$, then $\lim_{t \to \infty} x(t) = 0$ for every solution $x(t)$ of (20).*
(b) *If $h'_a(0) < -1$, then*

$$\alpha \leq \alpha_1 \leq \liminf_{t \to \infty} x(t) \leq \limsup_{t \to \infty} x(t) \leq \beta_1 \leq \beta,$$

for every solution $x(t)$ of (20), where $\{\alpha_1, \beta_1\}$ is the unique 2-cycle of h_a.

Notice that $h'_a(x) < 0$ if and only if $g'(x) > 0$, and $(Sh_a)(x) < 0$ if and only if $(Sg)(x) < 0$. We emphasize that Proposition 2 can be applied to the case of unimodal maps when the attracting invariant interval $[h_a(h_a(c)), h_a(c)]$ is included in the domain where h_a is decreasing, that is, if $h_a(h_a(c)) > c$.

Now we apply Proposition 2 to Eq. (5). In this case, the map $g(x) = 7\delta^2 e^{-\delta} \arctan(x)$ is bounded and

$$g'(x) = \frac{7\delta^2 e^{-\delta}}{1 + x^2} > 0, \quad (Sg)(x) = \frac{-14\delta^2 e^{-\delta}}{(1 + x^2)^2} < 0, \ \forall x \in \mathbb{R}.$$

Notice also that

$$h'_\delta(0) = \left(e^{-\delta} - 1\right) 7\delta e^{-\delta} < -1 \iff \delta \in J = (\delta_*, \delta^*) \approx (0.58, 2.99).$$

Fig. 5 Lower and upper bounds for the location of the bubble generated by Eq. (5) as δ is increased. As expected, the closed curve obtained from the numerical approximation of the minimum and the maximum of the attracting periodic solutions is located between the bounds
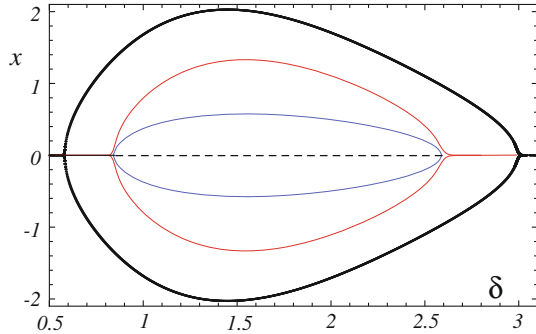
Thus, if $\{\alpha_1(\delta), \beta_1(\delta)\}$ is the unique 2-cycle of h_δ for each $\delta \in J$, then the set

$$\bigcup_{\delta \in J}(\delta, \alpha_1(\delta)) \cup \bigcup_{\delta \in J}(\delta, \beta_1(\delta))$$

forms a closed loop. It is the most exterior closed curve in Fig. 5.

The inner closed curve in Fig. 5 is obtained as

$$\bigcup_{\delta \in (\delta_1, \delta_2)}(\delta, -A(\delta)) \cup \bigcup_{\delta \in (\delta_1, \delta_2)}(\delta, B(\delta)),$$

where δ_1, δ_2 are the two Hopf bifurcation points for equation (5), and $A(\delta), B(\delta)$ are defined in (19). According to Theorem 1, Eq. (5) has no slowly oscillatory solutions contained in $(-A(\delta), B(\delta))$. The numerical approximation of the bubble obtained by plotting the minimum and the maximum of the attracting periodic orbits (see Fig. 3) is located in Fig. 5 between the lower and upper bounds.

6 Applications: The Mackey Equation and the Nicholson's Blowflies Equation

In this section we apply our results to well known equations. Our first example is the Mackey equation, which can be written as

$$x'(t) = -\delta x(t) + \frac{1}{1 + x^m(t - \tau)}, \tag{21}$$

where $x(t)$ is the circulating density of RBC at time t, δ is the destruction rate of RBC, m is a positive parameter estimated experimentally, and τ is a feedback delay (see [24] for more details). We consider the values $m = 7.6$ and $\tau = 1.73$ used in [24] (see also [9]).

Notice that the nonlinearity $h(x) = 1/(1 + x^m)$ is decreasing and thus complex behaviour in (21) is not possible [38]. It is clear that Eq. (21) has a unique positive equilibrium $k(\delta)$ determined by the unique positive solution of equation $x^{m+1} + x = 1/\delta$.

Fig. 6 Stability chart for the Mackey's equation (22) with $m = 7.6$ in the plane of parameters (a, τ). The *dashed line* corresponds to the parameter $\tau = 1.73$ used in [24]. The *numbers between the curves* indicate how many roots the characteristic equation has with positive real part (Thus, 0 corresponds to the stability region)
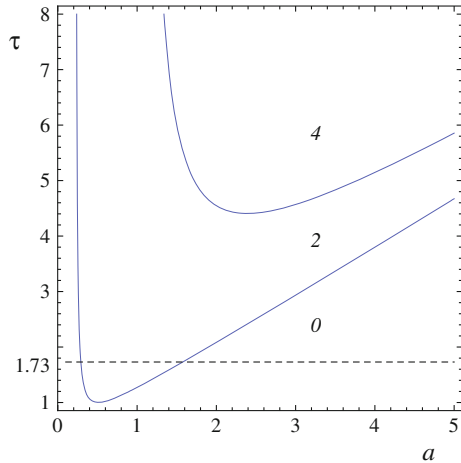
The change of variables $y(t) = x(\tau t) - k(\delta)$ transforms (21) into

$$y'(t) = -ay(t) - g(y(t-1)), \tag{22}$$

where $a = \delta\tau$ and

$$g(y) = \tau \left(\frac{1}{1 + (k(\delta))^m} - \frac{1}{1 + (y + k(\delta))^m} \right).$$

Mackey already observed the existence of two Hopf bifurcation points $a_1 \approx 0.289$, $a_2 \approx 1.576$, in such a way that 0 is asymptotically stable for $a < a_1$ and $a > a_2$, and it is unstable for $a \in (a_1, a_2)$. It is known that there is at least a slowly oscillatory periodic solution of (22) for all $a \in (a_1, a_2)$. Numerical simulations suggest that this periodic solution is unique (for further discussions, see [18,21]). In Fig. 6, we plot the stability chart for Eq. (22) with $m = 7.6$ in the plane of parameters (a, τ). For the considered value $\tau = 1.73$ and $a \in (a_1, a_2)$, the associated characteristic equation has exactly two roots with positive real part.

Theorem 1 can be applied to find a region where slowly oscillatory periodic solutions cannot exist. Define $b = (a^2 + \omega^2)^{1/2}$, where ω is the unique solution of $\omega = -a \tan(\omega)$ in $(\pi/2, \pi)$. For $a \in (a_1, a_2)$, equation $g'(y) = b$ has exactly one negative solution $-A(a)$, and one positive solution $B(a)$.

The inner closed curve we plot in Fig. 7 is delimited by the curves $m(a)$ and $-m(a)$, $a \in (a_1, a_2)$, where $m(a) = \min\{A(a), B(a)\}$. It is obvious from Theorem 1 that there are no slowly oscillatory periodic solutions of (22) y with $y(\mathbb{R}) \subset (-m(a), m(a))$.

Since the auxiliary map $h_a(x) = (e^{-a} - 1)g(x)/a$ is decreasing and has negative Schwarzian derivative (see, e.g., [21]), we can apply Proposition 2. The points a_0, a_3 where $h'_a(x) = -1$ are estimated numerically as $a_0 \approx 0.162$, $a_3 \approx 1.819$. The exterior closed curve in Fig. 7 is determined by the points $(a, \alpha_1(a))$, $(a, \beta_1(a))$, $a \in (a_0, a_3)$, where $\{\alpha_1(a), \beta_1(a)\}$ is the unique 2-cycle of h_a.

Fig. 7 Lower and upper bounds for the location of the bubble obtained from the Mackey equation (22) as the parameter a is increased
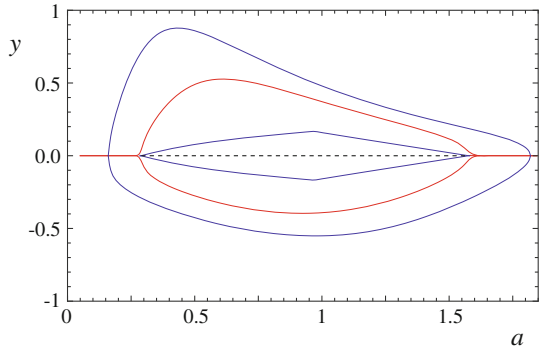
We also include in Fig. 7 a graphic representation of the bubble defined by (22); it was obtained plotting the numerical approximation of the minimum and the maximum of the attracting periodic orbit starting at an initial condition close to zero. As predicted by the analytical results, it is located between the lower and the upper bounds.

Remark 2 A similar bifurcation diagram for Eq. (21) is plotted in [9, Section 3.3], including an upper bound obtained by another approach. Such an upper bound is different from the one we got from Proposition 2; in particular, it does not have a *bubble shape,* so it does not predict the existence of two Hopf bifurcation points.

Our next example is the Nicholson's blowflies equation:

$$x'(t) = -\delta x(t) + px(t-\tau)e^{-\gamma x(t-\tau)}, \tag{23}$$

where δ, p, γ and τ are positive constants. We consider (23) as a model for the growth of an exploited population, and assume a strategy of harvesting based on constant effort, that is, the catch is proportional to the population size. Then, an increase in harvesting pressure can be seen as an increase in the mortality parameter δ in (23). This kind of strategy arises in the modelling of fisheries: a fixed number of boats is allowed to fish for some fixed interval of time; then, if the fish is distributed uniformly in the sea, the catch will be proportional to the stock density [4,5]. If we pursue to analyze the response of the system to harvesting, this means that we should study the changes in the behaviour of (23) when parameter δ is increased.

An important difference with the previous example is that the function $h(x) = pxe^{\gamma x}$ is unimodal, and this fact has important consequences in the dynamics of (23); in particular, complex behaviour is possible (see, e.g., [18, Section 4] and references therein).

It is known (see, e.g., [13,20,23]) that Eq. (23) has a unique equilibrium $x = 0$ if $\delta \geq p$, and it attracts all nonnegative solutions. If $\delta < p$, then there is a positive equilibrium $k(\delta) = (1/\gamma)\ln(p/\delta)$, and $x = 0$ becomes unstable. Moreover, $k(\delta)$ is globally attracting for all values of the delay if and only if $\delta \in [pe^{-2}, p)$. This means that, regardless the value of the delay, too large harvesting effort in (23) results in extinction, and this is explained mathematically by a global transcritical bifurcation at $\delta = p$.

Next, for $\delta < pe^{-2}$, $k(\delta)$ is globally asymptotically stable for all sufficiently small values of the delay (see, e.g., [13,23]). This indicates that the dynamics of (23) for small values of τ is essentially the same as the dynamics of the ordinary differential equation ($\tau = 0$), that is, an increasing mortality results in a decreasing globally attracting equilibrium (notice that $\partial k(\delta)/\partial \delta = -1/(\gamma\delta) < 0$).

The (local) stability analysis can be performed similarly to that of Eq. (2). Setting $y(t) = \gamma x(\tau t) - \gamma k(\delta)$ we obtain the equation

$$y'(t) = \delta\tau\left(-y(t) - g(y(t-1))\right) \tag{24}$$

with $g(y) = g(y, \delta, p) = \ln\left(\frac{p}{\delta}\right)(1 - e^{-y}) - ye^{-y}$.

The only equilibrium of (24) in $(-k(\delta), \infty)$ is $y = 0$. Since $g'(0) = \ln(p/\delta) - 1$, the characteristic equation associated to the variational equation of (24) about 0 is

$$\lambda + \delta\tau - \delta\tau\left(1 - \ln(p/\delta)\right)e^{-\lambda} = 0. \tag{25}$$

The border of the asymptotic stability of the equilibrium is given by the relation

$$\arccos\left(\frac{1}{1 - \ln(p/\delta)}\right) = \tau\delta\sqrt{(1 - \ln(p/\delta))^2 - 1}. \tag{26}$$

This expression allows us to represent the stability region of (24) in the plane of parameters $(\delta\tau, p\tau)$. The lower solid curve in Fig. 8 represents the boundary of the stability region for $\delta\tau \in (0, 30)$, $p\tau \in (0, 220)$. The other solid curves represent the values for which other branches of roots of (25) reach the imaginary axis, which are defined by the implicit equations

Fig. 8 Stability chart for the Nicholson's blowflies equation in the plane of parameters $(\delta\tau, p\tau)$. The *dashed lines* correspond to the cases of study: $\tau = 10$, $p = e^3$, and $\tau = 2$, $p = e^3$. The *numbers between the curves* indicate how many roots the characteristic equation has with positive real part
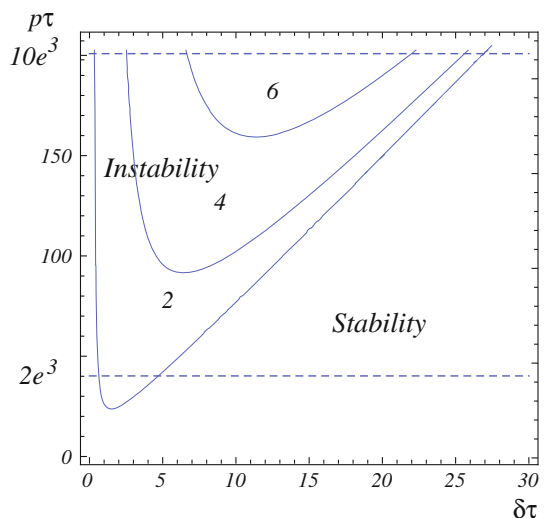
$$\arccos \left(\frac{1}{1 - \ln(p/\delta)}\right) + 2k\pi = \tau\delta\sqrt{(1 - \ln(p/\delta))^2 - 1}, \ k = 1, 2. \quad (27)$$

A Hopf bifurcation analysis for the Nicholson's blowflies equation (23) was done in [39], taking the delay τ as the bifurcation parameter. In this case, the authors prove that if $\lambda(\tau) = \alpha(\tau) + i\beta(\tau)$ is a root of (25) and $\alpha(\tau_*) = 0$, then $\alpha'(\tau_*) > 0$. Thus, it is impossible to get a bubble in the bifurcation diagram.

In the rest of the section, we present a case of study for Eq. (24) in order to illustrate the effects of increasing δ, and the influence of the length of the delay parameter τ.

From now on, we fix $p = e^3$, and assume $\delta < p$ to ensure the existence of a positive equilibrium. Thus, equation (24) writes

$$x'(t) = -\delta\tau x(t) - \delta\tau \left((3 - \ln(\delta)) \left(1 - e^{-x(t-1)}\right) - x(t-1)e^{-x(t-1)}\right). \quad (28)$$

The unique equilibrium of (28) in $(\ln(\delta)/3 - 1, \infty)$ is $x = 0$. For $\delta \in [e, e^3)$, it is globally asymptotically stable for all values of the delay.

As discussed before, for $\tau = 0$ the equilibrium is globally attracting for all $\delta \in (0, e^3)$. Using the global stability Theorem 2.1 in [23], it follows that the same trivial dynamics holds for $\tau < \tau_1 \approx 1.18117$.

We next combine some numerical experiments with our theoretical results to illustrate how an increase in the mortality rate δ can enhance variability in the asymptotic behaviour of the solutions of (28). When τ is small, complex behaviour is not observed and our simulations, together with Theorem 2, suggest existence of bubbles. For larger values of τ, our numerical experiments show an increasing complex behaviour after the first bifurcation point, followed by convergence to periodic orbits, and a stable equilibrium again after the second bifurcation point. Despite the complex behaviour observed for some values of the parameters, it seems that bubbles in the sense of Definition 1 are still present.

First, let us take $\tau = 2$, so Eq. (28) writes

$$y'(t) = -ay(t) - g(y(t-1)), \quad (29)$$

where $a = 2\delta$ and

$$g(y) = a\left[(3 - \ln(a/2))\left(1 - e^{-y}\right) - ye^{-y}\right].$$

The bifurcation points $a_1 \approx 0.63$, $a_2 \approx 4.7$ can be calculated using the relation (26). Our simulations show that this value of the delay is small enough to prevent complex behaviour, and all solutions converge either to 0 (if $a < a_1$ or $a > a_2$), or to a slowly oscillatory periodic solution (if $a \in (a_1, a_2)$).

Since function g is unimodal and has negative Schwarzian derivative (see, e.g., [13,23]), to get un upper bound for the location of the bubble, we will make use of Propositions 1 and 2. It is easy to check that the auxiliary map

$$h_a(y) = \frac{e^{-a} - 1}{a}g(y) = \left(e^{-a} - 1\right)\left[(3 - \ln(a/2))\left(1 - e^{-y}\right) - ye^{-y}\right]$$

Fig. 9 Graphic representation of the bubble obtained from the Nicholson's blowflies equation (29) as the parameter a is increased, together with the lower and upper bounds coming from the analytical results
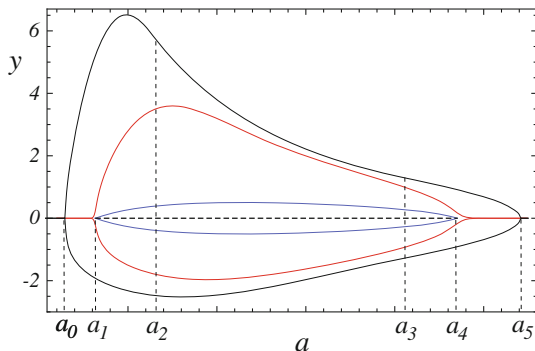
has a unique local maximum at $c_a = \ln(a/2) - 2$. We can find numerically the points for which $h'_a(0) = -1$, and those satisfying $h_a(h_a(c_a)) = c_a$. On the one hand,

$$h'_a(0) < -1 \iff a \in (a_0, a_5) \approx (0.295, 5.412).$$

On the other hand, equation $h_a(h_a(c_a)) = c_a$ has exactly two solutions on (a_0, a_5), given by $a_2 \approx 1.26$ and $a_3 \approx 4.107$. Moreover, $h_a(h_a(c_a)) > c_a$ for $a \in (a_0, a_2) \cup (a_3, a_5)$, and $h_a(h_a(c_a)) < c_a$ for $a \in (a_2, a_3)$. This means that h_a is monotone decreasing on the attracting interval $[h_a(h_a(c_a)), h_a(c_a)]$ for $a \in (a_0, a_2) \cup (a_3, a_5)$. Thus, Propositions 1 and 2 allow us to get bounds for the maximum and the minimum of the solutions. They are represented in Fig. 9, respectively, by the curves

$$\left(\bigcup_{a \in (a_0, a_2) \cup (a_3, a_5)} (a, \beta_1(a)) \right) \cup \left(\bigcup_{a \in (a_2, a_3)} (a, h_a(c_a)) \right)$$

and

$$\left(\bigcup_{a \in (a_0, a_2) \cup (a_3, a_5)} (a, \alpha_1(a)) \right) \cup \left(\bigcup_{a \in (a_2, a_3)} (a, h_a(h_a(c_a))) \right),$$

where, for each $a \in (a_0, a_2) \cup (a_3, a_5)$, $\{\alpha_1(a), \beta_1(a)\}$ is the unique 2-cycle of h_a.

Next we apply Theorem 1. If ω is the unique solution of $\omega = -a \tan(\omega)$ in $(\pi/2, \pi)$, and $b = (a^2 + \omega^2)^{1/2}$, then for each $a \in (a_1, a_4) \approx (0.63, 4.7)$, equation $g'(y) = b$ has exactly one negative solution $-A(a)$, and one positive solution $B(a)$, with $B(a) < A(a)$. Thus Theorem 1 ensures that (29) has no slowly oscillatory periodic solutions y with $y(\mathbb{R}) \subset (-B(a), B(a))$.

The parametric curves $(a, -B(a)), (a, B(a))$ for $a \in (a_1, a_4)$ provide the inner closed curve in Fig. 9. As in the previous examples, the approximations of the minimum and the maximum values of the attracting periodic solutions provide a representation of the bubble located inside the region determined by the lower and the upper bounds.

Fig. 10 Numerical approximation of the minimum norm of the segments x_t of a solution of (28) with $\tau = 10$ and $\delta \in (0, 4)$, suggesting a bubbling shape
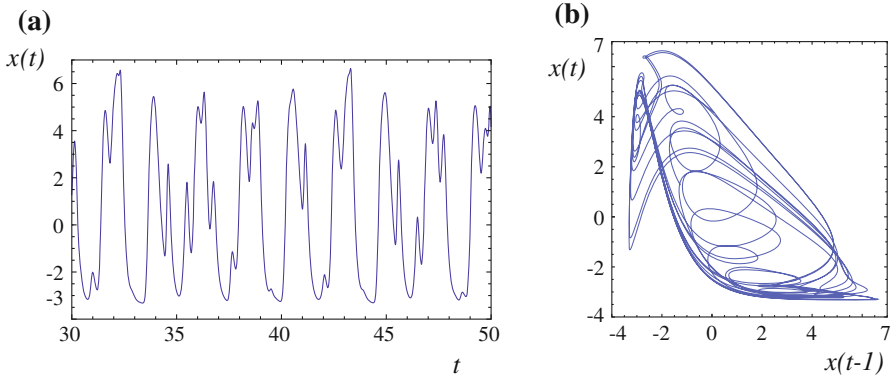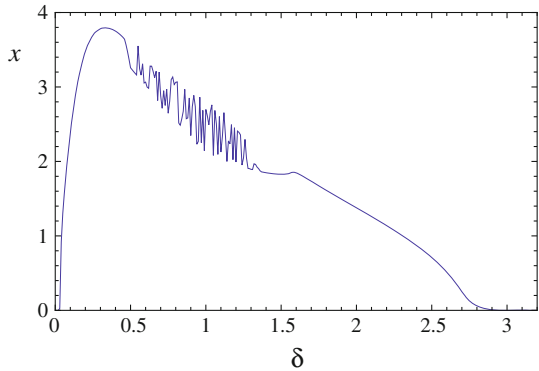

Fig. 11 Solution of (28) with $\tau = 10$, $\delta = 0.7$: (**a**) $x(t)$ versus t; (**b**) $x(t)$ versus $x(t-1)$

Next we consider Eq. (28) with $\tau = 10$, where more complex behaviour is observed for some values of δ. As before, the bifurcation points where the positive equilibrium changes its stability can be calculated numerically using the relation (26). This provides the values $\delta_1 \approx 0.033$, $\delta_2 \approx 2.701$.

In Fig. 10 we plot, for $\delta \in (0, 3)$, an approximation of the minimum norm of the segments of a solution $x(t)$ of (28) with $\tau = 10$, which suggests that it is bounded away from zero, giving rise to a bubble in the sense of Definition 1. Other numerical experiments for different initial conditions provide similar figures.

The range of values δ for which the curve is more abrupt may correspond to more complex dynamics. However, as far as we know, no results are available to explain this phenomenon. In Fig. 11 we plot a numerical solution of (28) with $\delta = 0.7$, $\tau = 10$, and a projection of its orbit over the plane $(x(t-1), x(t))$.

The limit form of Eq. (28) as $\tau \to \infty$ is the difference equation with continuous argument

$$x(t) = -(3 - \ln(\delta))\left(1 - e^{-x(t-1)}\right) + x(t-1)e^{-x(t-1)} := h(\delta, x(t-1)),$$

Fig. 12 Bifurcation diagram of (30) with $\delta \in (1, 3)$
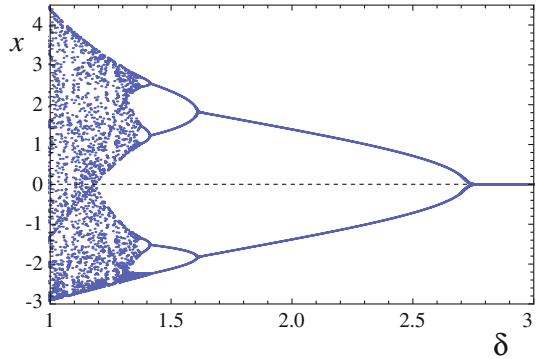
whose dynamics is governed by the one-dimensional discrete equation of Ricker type [36]

$$x_{n+1} = h(\delta, x_n). \tag{30}$$

In Fig. 12, we show the bifurcation diagram corresponding to (30) with $\delta \in (1, 3)$. The dashed line denotes the unstable equilibrium.

We notice that, if $\delta_1(\tau)$, $\delta_2(\tau)$ denote, respectively, the points at which the equilibrium of (28) loses and recovers its asymptotic stability, then $\lim_{\tau \to \infty} \delta_1(\tau) = 0$, $\lim_{\tau \to \infty} \delta_2(\tau) = e$. For the limiting Eq. (30), there are no bubbles, and increasing the mortality rate δ helps to stabilize the equilibrium. Actually, the equilibrium becomes globally stable after a period-halving bifurcation at $\delta = e$.

In conclusion, the main finding of our analytical and numerical study of the possible destabilizing effect of increasing mortality in Nicholson's blowflies delay differential equation (23) is the following: as it is well known, for small values of τ, the dynamics is as simple as in the nondelayed case; thus increasing mortality does not destabilize the positive equilibrium. For larger values of τ the dynamics is still simple, but an increment of parameter δ leads to a bubble, thus inducing oscillations between the two Hopf-bifurcation points. For even larger values of τ, increasing mortality induces instabilities, and the dynamics seems to become more complex; further harvesting effort leads to an attracting equilibrium again. Finally, for the limit case $\tau = \infty$, increasing mortality tends to simplify the dynamics from a chaotic behaviour to a globally stable equilibrium via period-halving bifurcations.

References

1. Ambika, G., Sujatha, N.V.: Bubbling and bistability in two parameter discrete systems. Pramana J. Phys. **54**, 751–761 (2000)
2. Anderson, C.N.K. et al.: Why fishing magnifies fluctuations in fish abundance. Nature **452**, 835–839 (2008)
3. Bier, M., Bountis, T.C.: Remerging Feigenbaum trees in dynamical systems. Phys. Lett. A **104**, 239–244 (1984)
4. Brauer, F., Castillo-Chávez, C.: Mathematical Models in Population Biology and Epidemiology. Springer, New York (2001)
5. Clark, C.W.: Mathematical bioeconomics: the optimal management of renewable resources, 2nd edn. Wiley, Hoboken (1990)
6. Cooke, K., van den Driessche, P., Zou, X.: Interaction of maturation delay and nonlinear birth in population and epidemic models. J. Math. Biol. **39**, 332–352 (1999)
7. Dennis, B., Desharnais, R.A., Cushing, J.M., Costantino, R.F.: Transitions in population dynamics: equilibria to periodic cycles to aperiodic cycles. J. Anim. Ecol. **66**, 704–729 (1997)
8. Diekmann, O., Van Gils, S.A., Verduyn Lunel, S.M., Walther, H.-O.: Delay equations, functional-, complex-, and nonlinear analysis. Applied Mathematical Sciences. Springer, New York (1995)
9. Erneux, T.: Applied Delay Differential Equations. Springer, New York (2009)
10. Foley, C., Mackey, M.C.: Dynamic hematological disease: a review. J. Math. Biol. **58**, 285–322 (2009)
11. Glass, L., Mackey, M.C.: Pathological conditions resulting from instabilities in physiological control systems. Ann. New York Acad. Sci. **316**, 214–235 (1979)
12. Gurney, W.S.C., Blythe, S.P., Nisbet, R.M.: Nicholson's blowflies revisited. Nature **287**, 17–21 (1980)
13. Győri, I., Trofimchuk, S.: Global attractivity in $x'(t) = -\delta x(t) + p f(x(t-\tau))$. Dyn. Syst. Appl. **8**, 197–210 (1999)
14. Hale, J.K.: Asymptotic Behavior of Dissipative Systems. American Mathematical Society, Providence (1988)
15. Hale, J.K., Verduyn Lunel, S.M.: Introduction to Functional Differential Equations. Springer, New York (1993)
16. an der Heiden, U., Mackey, M.C.: The dynamics of production and destruction: analytic insight into complex behavior. J. Math. Biol. **16**, 75–101 (1982)
17. Krisztin, T.: Periodic orbits and the global attractor for delayed monotone negative feedback. Electron. J. Qual. Theory Differ. Equ. (2000). In: Proceedings of the 6th Colloquium on the Qualitative Theory of Differential Equations (Szeged, 1999), vol. 15, pp. 1–12
18. Krisztin, T.: Global dynamics of delay differential equations. Period. Math. Hungar. **56**, 83–95 (2008)
19. Kuang, Y.: Delay Differential Equations with Applications in Population Dynamics. Academic Press, Boston (1993)
20. Liz, E., Röst, G.: On the global attractor of delay differential equations with unimodal feedback. Discrete Contin. Dyn. Syst. **24**, 1215–1224 (2009)
21. Liz, E., Röst, G.: Dichotomy results for delay differential equations with negative Schwarzian derivative. Nonlinear Anal. Real World Appl. **11**, 1422–1430 (2010)
22. Liz, E., Ruiz-Herrera, A.: The hydra effect, bubbles, and chaos in a simple discrete population model with constant effort harvesting. J. Math. Biol. (accepted)
23. Liz, E., Tkachenko, V., Trofimchuk, S.: A global stability criterion for scalar functional differential equations. SIAM J. Math. Anal. **35**, 596–622 (2003)
24. Mackey, M.C.: Periodic auto-immune hemolytic anemia: an induced dynamical disease. Bull. Math. Biol. **41**, 829–834 (1979)
25. Mackey, M.C., Glass, L.: Oscillation and chaos in physiological control systems. Science **197**, 287–289 (1977)
26. Mackey, M.C., Milton, J.G.: Dynamical diseases. Ann. N. Y. Acad. Sci. **504**, 16–32 (1987)
27. Mallet-Paret, J., Nussbaum, R.: Global continuation and asymptotic behaviour for periodic solutions of a differential-delay equation. Ann. Mat. Pura Appl. **145**, 33–128 (1986)
28. Mallet-Paret, J., Sell, G.R.: The Poincaré-Bendixson theorem for monotone cyclic feedback systems with delay. J. Differ. Equ. **125**, 441–489 (1996)
29. Mallet-Paret, J., Walther, H.-O.: Rapid oscillations are rare in scalar systems governed by monotone negative feedback with a time delay. Preprint (1994)

30. May, R. M.: Mathematical models in whaling and fisheries management. In: Some Mathematical Questions in Biology (Proc. 14th Sympos., San Francisco, Calif., 1980), pp. 1–64. Lectures Math. Life Sci., vol. 13. Amer. Math. Soc., Providence
31. May, R.M.: Nonlinear phenomena in ecology and epidemiology. Ann. N. Y. Acad. Sci. **357**, 267–281 (1980)
32. May, R.M., Beddington, J.R., Horwood, J.W., Shepherd, J.G.: Exploiting natural populations in an uncertain world. Math. Biosci **42**, 219–252 (1978)
33. Nicholson, A.J.: An outline of the dynamics of animal populations. Austral. J. Zool. **2**, 9–65 (1954)
34. Nisbet, R.M.: Delay-differential equations for structured populations. In: Structured-Population Models in Marine, Terrestrial, and Freshwater Systems, pp. 89–118. Population and Community Biology Series, vol. 18. Chapman & Hall, New York (1997)
35. Smith, H.L.: An Introduction to Delay Differential Equations with Applications to the Life Sciences. Texts in Applied Mathematics, vol. 57. Springer, New York (2011)
36. Thieme, H.R.: Mathematics in Population Biology. Princeton University Press (2003)
37. Walther, H.-O.: A theorem on the amplitudes of periodic solutions of differential delay equations with applications to bifurcation. J. Differ. Equ. **29**, 396–404 (1978)
38. Walther, H.-O.: The 2-dimensional attractor of $x'(t) = -\mu x(t) + f(x(t-1))$. Mem. Am. Math. Soc., vol. 544. American Mathematical Society, Providence (1995)
39. Wei, J., Li, M.Y.: Hopf bifurcation analysis in a delayed Nicholson blowflies equation. Nonlinear Anal. **60**, 1351–1367 (2005)
40. Zipkin, E.F., Kraft, C.E., Cooch, E.G., Sullivan, P.J.: When can efforts to control nuisance and invasive species backfire. Ecol. Appl. **19**, 1585–1595 (2009)